

# A LINEAR CELLULAR AUTOMATION TECHNIQUE FOR PREDICTING DYNAMIC FAILURE MODE OF A SINGLE-LAYER SHELL

M. Zhang<sup>1,2</sup> - Y. Zhang<sup>1,2</sup> - Y. X. Huang<sup>1,2</sup> - G. C. Zhou<sup>1,2\*</sup> - Z. T. Jing<sup>3</sup>

<sup>1</sup>Key Lab of Structures Dynamic Behavior and Control (Harbin Institute of Technology), Ministry of Education, Heilongjiang, Harbin, 150090, China

<sup>2</sup>School of Civil Engineering, Harbin Institute of Technology, Heilongjiang, Harbin, 150090, China

<sup>3</sup>Beijing Institute of Architectural Design, Nanlishi Rd.62, Beijing, 100045, China

## ARTICLE INFO

### Article history:

Received: 04.09.2013.

Received in revised form: 20.09.2013.

Accepted: 02.10.2013.

### Keywords:

Linear cellular automation

The single-layer latticed shell

The cylindrical latticed shell

Dynamic failure mode

Nodal domain

Criterion

## Abstract:

*This paper presents a linear cellular automation (LCA) method for predicting the dynamic failure (DF) mode of both single-layer latticed shell and single-layer cylindrical latticed shell subjected to ground motions. The LCA model of the shell obtains the state values of cells/nodes including the nodal displacements state value and the nodal domain logarithmic strain energy density (NDLSED) state value through its finite element analysis (FEA). Meanwhile, the concepts of nodal domain and nodal domain similarity are derived based on the qualitative analysis of shells. Then, similar nodal domains between two shells are matched through the proposed criterion. Finally, the DF mode of an object shell is mapped using the criterion for projecting the formative values of a base shell to similar nodal domains in the object shell. Case studies show that the LCA method could be used for predicting the DF mode of an object shell. Consequently, the LCA method would explore an LCA application in analyzing shells, which costs much less time than the FEA method for calculating the DF shell mode.*

## 1 Introduction

The latticed shell structures develop rapidly all over the world due to their aesthetic qualities, large space and sound mechanical performance. An outstanding example is that the latticed shells successfully survived during the 1995 destructive Kobe earthquake in Japan, which clearly demonstrated excellent seismic performance. [1]. This further aroused researchers' interest in the analysis of shell

structures under dynamic loads. Early thin shell structures might have been empirical and conceptual products constructed by human bionic practice. Then, a remarkable performance of this type of structures has led to the construction of many modern large span shell structures around the world. Recently, the development of construction materials, advanced analytical methods and modern construction techniques seems to have encouraged a wide use of this type of structures, particularly in

\* Corresponding author. Tel.: (+86)451-86283199;  
E-mail address: gzhou@hit.edu.cn

the seismic areas. However, the following issues still need to be addressed:

(1) A hot issue is to identify and model the failure mechanism of large-span single-layer shells under the strong seismic loading [2-4]. Commonly, structural instability is believed to be the main cause of failure in shell structures subjected to seismic excitations. But, structural instability is so complex in its mechanism that it is difficult to determine the corresponding load and mode [5].

(2) The finite element analysis (FEA) is widely used in structural analysis and design at present. But, the FEA computation of shell structures undergoing whole seismic processes costs a lot of time, particularly, the post-processing of huge calculation data. Hence, alternative convenient and highly efficient methods are expected to address the computing cost.

(3) As Kunieda and Kitamura [1] indicated, the analysis of shell structure is still needed to verify whether the existing shell structures were too strongly designed, or not.

(4) The existing design codes around the world also lack sufficient guidance to support a confident and reliable design approach.

(5) Results obtained from FEA simulations and tests of shells ought to be further investigated or modeled to discover new knowledge.

In view of the issues mentioned above, an exploration of both modeling and predicting methods is needed to further new analytical techniques, to apply the test and numerical results and to reduce the computing time of shell structures. Zhou et al. [6] successfully tried and met this expectation in mapping the cracking pattern of masonry wall panels using cellular automata, which provides a reference basis for predicting the dynamic failure (DF) modes of shells.

This paper conducts a linear cellular automaton (LCA) modeling of a shell structure, because the shell structure itself is a latticed form and the structural nodes are similar to cells in a LCA model. Thus, it is appropriate to develop the concepts of nodal domain and nodal domain similarity, as well as the criteria for matching nodal domain similarity for shell structures. Finally, the LCA method is proposed to predict the DF modes of object shell structures based on the DF mode of a based shell.

## 2 Concepts proposed in the LCA method

Based on the cellular automata developed by Neuman [7], Margolus and Toffoli [8], the concepts for the LCA method are introduced as follows:

**Nodal domain:** A node and its six neighbouring nodes are defined as a nodal domain, as shown in Fig. 1. **Nodal state value:** The normalized FEA displacements of all nodes are defined as nodal state values, for the shell under a unit load (here, the amplitude of acceleration equaling  $0.1\text{m/s}^2$  is regarded as the unit load). In other words, nodal state values are set as the state values of any cells in the LCA model of the shell.

**Nodal domain similarity:** It is defined as nodal domain similarity when two nodes with their neighbourhoods have the same or similar node state values [6, 9].

**DF mode:** the DF mode is composed of all the normalized nodal displacements or nodal domain logarithmic strain energy density (NDLSED) once the shell has become unstable.

**Base shell:** A typical shell whose DF mode is known from the FEA numerical simulation result or testing data. The normalized DF mode provides a basis or reference for predicting the DF mode of an object shell.

**Object shell:** A shell whose DF mode needs to be predicted. Here, the FEA numerical simulation results of the object shell are available to verify the LCA method.

## 3 Database preparation

### 3.1 Verification of the FEA program

Testing and FEA models are shown in Fig. 2. Details of the testing process are not shown due to the page limits. The lab test of the shell model was

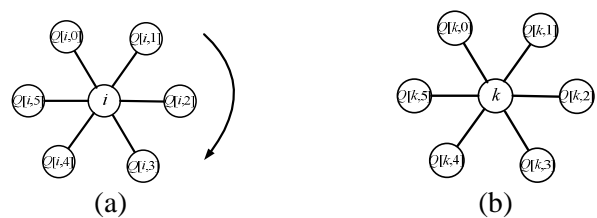


Figure 1. Nodes in the nodal domain; (a) the  $i$ th node and its neighbourhoods in the object shell, (b) the  $k$ th node and its neighbourhoods in the base shell.

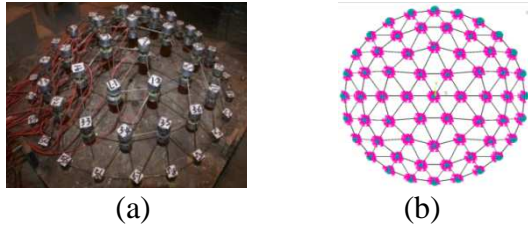


Figure 2. The testing & FEA Shell Models; (a) The testing model, (b) The FEA model.

Table 1. The testing and FEA frequencies.

	Test model	FEA model	Error
$f_1$	22.16	22.18	0.09
$f_2$	24.29	24.12	0.69

conducted in the structural and earthquake-resistant testing center of the school of civil engineering at Harbin Institute of Technology in order to validate the FEA program. Table 1 lists the first and second natural frequencies ( $f_1, f_2$ ) obtained from the testing and the FEA simulation. Table 1 indicates that the FEA frequencies are very close to the lab testing ones.

### 3.2 Database

After validating the FEA program, the database for shells shown in Fig. 3 is established as a basic component for the LCA method. The database consists of two parts:

- (1) The normalized FEA results of the base and object shells under unit loading case;
- (2) The normalized FEA (or testing) nodal displacements and NDLSSED once the base shell has become instable.

## 4 The proposed LCA method

### 4.1 The LCA model of the shell

The shell can be constructed as a LCA model. The LCA is a subclass of cellular automata consisting of a lattice of sites on a cylinder evolving according to a linear local interaction rule [10]. The shell nodes could be considered as the cells of the LCA model. The time and spatial expression of the LCA model is set to correspond to the sections (1) and (2):

- (1) The linear relationship exists between seismic intensity and displacement response of the shell before its plastic state. The nodal displacement of

the shell with viscous damping under harmonic excitations [11] can be expressed as Eq. (1):

$$\{u(t)\} = \frac{P_0}{K_n} \sum_{n=1}^N A_n \{\phi\}_n \sin(\omega t + \varphi_n) \quad (1)$$

where  $A_n$  is a constant;  $P_0$  is loading amplitude;  $K_n$  is generalized stiffness. If the excitation is in the same seismic wavelength but with different amplitudes,  $P_{01}$  and  $P_{02}$ , the ratio of the nodal displacements corresponding to two different seismic amplitudes can be given as Eq. (2):

$$\frac{u_1(t)}{u_2(t)} = \frac{P_{01}}{P_{02}} \sum_{n=1}^N \frac{\sin(\omega t + \varphi_1)}{\sin(\omega t + \varphi_2)} \quad (2)$$

if  $\varphi_1 = \varphi_2$ , then  $\frac{u_1(t)}{u_2(t)} = \frac{P_{01}}{P_{02}} = \{k_1 \quad k_2 \quad \dots \quad k_n\}^T$

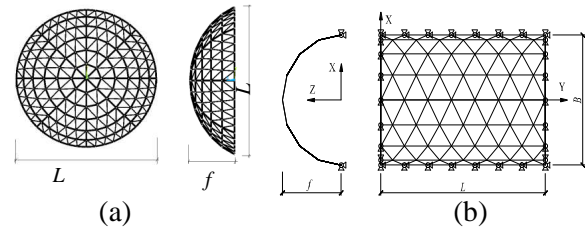


Figure 3. The FEA model of the shell; (a) The single-layer latticed shell, (b) The single-layer cylindrical latticed shell.

Eq. (2) indicates that all nodal displacements are linearly related to the amplitude of ground motion, coinciding with the linear property in the LCA mode of the shell. Thus, a node in the state  $I(i+1)$  can be updated by itself and its neighbourhoods in the state  $I(i)$ :

$$\{S\}_{I(i+1)}^{n \times 1} = [T]^{n \times n} \{S\}_{I(i)}^{n \times 1} \quad (3)$$

where  $\{S\} = \{a_0, a_1, \dots, a_n\}^T$  is the state vector of

the LCA cells;  $[T] = \begin{bmatrix} k_1 & 0 & \dots & 0 \\ 0 & k_2 & \dots & 0 \\ \vdots & \vdots & \ddots & \vdots \\ 0 & 0 & \dots & k_n \end{bmatrix}^{n \times n}$  is a

constant transformation matrix;  $I(i+1)$  and  $I(i)$  are two adjacent seismic intensities.

(2) The spatial property of the LCA model has existed in the database in which the fine FEA simulation has given out an implicit relationship between a cell and its neighbourhoods.

Actually, Eq. (3) also embodies three LCA properties, parallelism, locality and homogeneity. For the property of parallelism, the state values of individual cells can be synchronously updated. For the property of locality, the state value of a cell depends on the state values of itself and neighbouring cells. For the property of homogeneity, the same rules can be applied to each cell.

#### 4.2 The LCA state value

For nodal displacements, the cell state value in the LCA state mode is given as Eq. (4):

$$S_i = \frac{u_i^s}{\max(u_i^s)}, \quad i = 1, 2, L, N \quad (4)$$

where  $S_i$  is the  $i$ th nodal (or cell) state value;  $u_i^s$  is the  $i$ th nodal displacement under the unit load calculated by the FEA;  $\max(u_i^s)$  is the maximum among all the nodal displacements;  $N$  is the nodal number.

The NDLSSED is defined as a nodal domain normalization parameter of the logarithmic strain energy density. For the  $i$ th nodal domain shown in Fig. 4, the computational processes can be described as follows:

The strain energy of the element connected to the  $i$ th node is given by:

$$E_i = \frac{1}{2} \sum_{j=1}^N \{\sigma\}^T \{\varepsilon^{el}\} v_j + E_e^{pl} \quad (5)$$

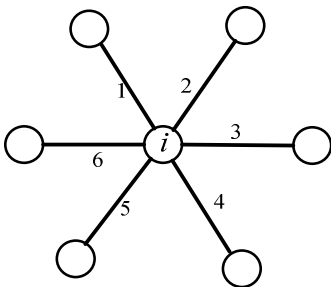


Figure 4. The  $i$ th nodal domain of single-layer shell.

where  $E_i$  is the strain energy of the  $i$ th element;  $N$  is the number of integration points;  $\{\sigma\}$  is the stress vector;  $\{\varepsilon^{el}\}$  is the elastic strain vector;  $v_j$  is the volume of the  $i$ th integration point;  $E_e^{pl}$  is the plastic strain energy.

Then, the strain energy density of the  $i$ th element and the strain energy density of the  $i$ th nodal domain can be determined:

$$I_j^i = \frac{E_j}{V_j} \quad (6)$$

$$I_i = \sum_{j=1}^6 I_j^i \quad (7)$$

where  $I_j^i$  is the strain energy density of the  $j$ th element in the  $i$ th nodal domain;  $I_i$  is the strain energy density of the  $i$ th nodal domain.

The NDLSSED is

$$S_i = \frac{\log(I_i)}{\max_{i=1}^N [\log(I_i)]} \quad i = 1, 2, L, N \quad (8)$$

where the  $\max_{i=1}^N [\log(I_i)]$  is the maximum of the  $N$  nodal domain logarithmic strain energy density in the single-layer shell.

#### 4.3 The criterion for matching nodal domain similarity

For all the nodal domains in the base shell or the object shell, the criterion for matching nodal domain similarity is given by Eq. (9)

$$E_i(k, e, j) = \min_{k=1}^{N_{\text{base}}} \left\{ \left\{ \min_{j=1}^5 \left[ \left[ |S[i] - S[k]| + \sum_{e=1}^{N_{\text{object}}} (S[Q(i, e-j)] - S[Q(k, \text{rem}(e, 6))]) \right] \right] \right\} \right\} \quad (9)$$

where  $S[i]$  refers to the  $i$ th nodal state values;  $Q$  refers to the neighbour nodes of a node;  $N_{\text{object}}$  and  $N_{\text{base}}$  are the nodal numbers of the object and base shells, respectively;  $\text{rem}(e, 6)$  is the remainder of the integer variables  $e$  and a constant integer 6 (the nodal number for a nodal domain).  $E_i(k, e, j)$  represents two processes:

- (1) Finding the minimum of the state value errors corresponding to six different orientations of two nodal domains, as shown in Fig. 1;
- (2) Finding the minimum of the state value errors between one nodal domain in the object shell and

all the nodal domains in the base shell. Thus, each nodal domain in the object shell can find its similar nodal domain on the base domain.

#### 4.4 The criterion for projecting state values of DF mode

When the failure of the base shell occurs, the normalized nodal displacements  $u_{base}^f$  or NDLSSED  $\log(I_i)$  are called as the formative values of DF mode and all of them are composed of the DF mode of the shell. Thus, a criterion can be given to project the formative values of the base shell to the similar nodes in the object shell, as shown by Eq. (10):

$$u_{object}^f(i) \Leftarrow u_{base}^f(k), \quad i=1,2,\dots,N_{object}, \quad k=1,2,\dots,N_{base} \quad (10)$$

where  $u_{object}^f(i)$  is the formative value of the  $i$ th nodal on the object shell.  $u_{base}^f(k)$  is the formative value of the  $k$ th nodal on the base shell. Eq. (10) means that the formative values  $u_{base}^f(i)$  on the base shell are assigned to the similar nodes in the object shell. Furthermore, all the formative values  $u_{object}^f(i)$  of the nodes on the object shell are normalized again by Eq. (11):

$$f^{object}(i) = \frac{u_{object}^f(i)}{\max_{j=1}^{N_{object}} [u_{object}^f(j)]} \quad (11)$$

Finally, all the normalized formative values  $f^{object}$  are composed of the DF mode of the object shell.

#### 4.5 The LCA procedure

Based on the LCA model of the shell, the method can be established to predict the DF mode of the object shell. Fig. 5 shows the procedure of the LCA method:

Step1. Build the LCA models for both object and base shells. Then, the state values in the LCA models are obtained from the database;

Step2. Find the nodal similarity domains between the base and object shells, using the state values obtained and the rule given by Eq. (9);

Step3. Construct the DF mode of the base shell utilizing the displacement values at the instability state of the shell;

Step4. Map the DF mode of the object shell through a criterion given by Eq. (10).

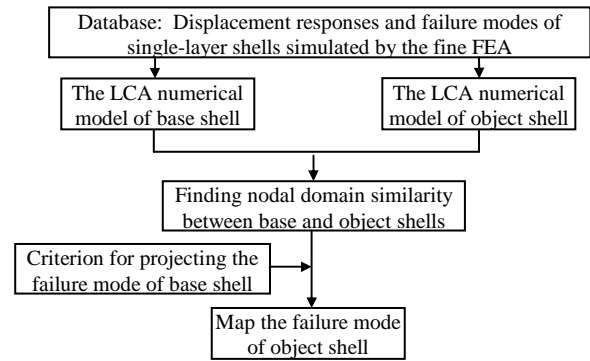


Figure 5. The LCA method for predicting the DF mode of single-layer shell.

### 5 Similarity between DF modes

Eq. (12) below is introduced to evaluate the similarity between the DF modes of the base and object shells. In other words, Eq. (12) is used to verify the accuracy of the LCA method:

$$\eta = 1 - \frac{1}{E} \sum_{i=1}^n |f_i^T - f_i^P|, \quad i=1,2,\dots,n \quad (12)$$

where  $\eta$  is the similarity;  $E = \sum_{i=1}^n |f_i^T + f_i^P|$ ;  $f_i^T$  refers to the  $i$ th nodal formative value of the object shell from the FEA or testing data;  $f_i^P$  represents the  $i$ th nodal formative value predicted by the LCA method;  $n$  is the number of the nodes in the object shell.

### 6 Numerical examples

Figures 6 and 7 give out the calculating results of the shells using the LCA method and the fine FEA method. Figure 6 shows the dynamic instability mode of single-layer latticed shell under harmonic ground motion. Figure 7 shows the dynamic strength failure mode of the single-layer cylindrical latticed shell under TAFT wave. Two cases are considered as:

Case 1. The DF mode of a base shell is used to predict the DF mode of the object shells with different configurations, for the same dynamic loading case;

Case 2. The DF mode of the base shell under a seismic frequency is used to predict the DF mode of the same shell under different seismic frequencies. From Fig. 6 and Fig. 7, it can be seen:

(1) The DF modes of the object shells predicted by the LCA method are very close to those simulated by fine FEA models;

(2) The average similarity in these examples is 91.26%;

(3) The normalized displacements of both base and object shells in their DF states are also close to each other. More examples are not shown here due to space constraints;

(4) The LCA method (5sec) spends much less computing time than that taken by the fine FEA simulation (more than 160h), as verified by the Big-O notation [13].

For the LCA method:

$$T(n) = O(n^2) \tag{13}$$

For the FEA method:

$$T(n_e) = n_1 \times n_2 \times n_3 \times n_4 \times n_5 \times n_6 = O((n_e)^6) \tag{14}$$

where  $n$  is the nodal number,  $n_1$  is the iterative number of mechanical constitutive relations for materials;  $n_2$  is the integral point on the cross section of the elements;  $n_3$  is the number of elements;  $n_4$  is the maximal substeps in each step of the input seismic wave;  $n_5$  is the input number of the seismic wave;  $n_6$  is the change number of the amplitude of the seismic wave.

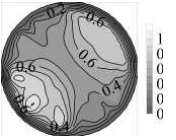
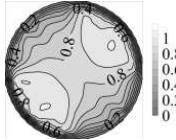
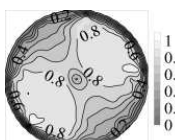
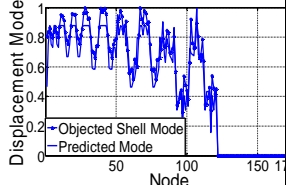
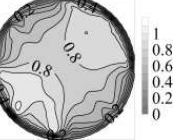
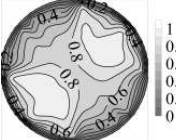
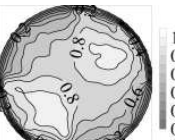
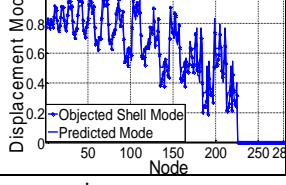
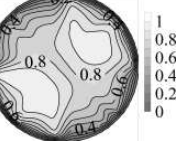
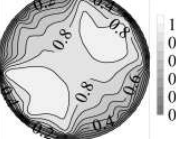
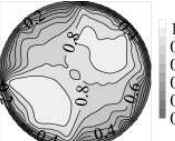
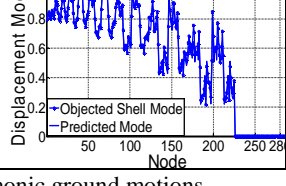
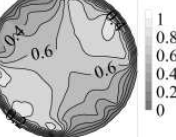
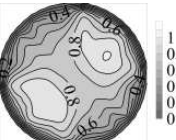
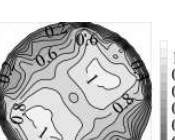
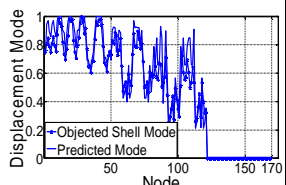
The dynamic instability mode of the base shell	The dynamic instability mode of the object shell	The dynamic instability mode of the object shell predicted by LCA method	Displacements of object and predicted shells	Similarity
The base and object shells have different ratios of rise-span.				
 D40205 Computing time: 168h	 D40203 Computing time: 160h	 Computing time: 5sec		94.69%
The base and object shells have different spans.				
 D50203	 D60203			96.35%
The base and object shells have different member cross-sections.				
 D60203a	 D60203b			98.20%
The base and object shells undergo different frequencies of harmonic ground motions.				
 D40203 (Loading frequency 5Hz)	 D40203 (Loading frequency 2Hz)			94.04%
Note	The shell is notated based on its span (m), roof weight ( $\times 10\text{kg/m}^2$ ) and ratio of span-rise. For D40203a, D: shell span (40 m), 20: the roof weight (200 $\text{kg/m}^2$ ), 3: the ratio of the span-rise, a: the cross section of the member. CPU: i5-2000@ 2.8GHz; Memory: 1.48GHz, 3.24GB			

Figure 6. The dynamic instability modes of shells and comparison of mode similarity.

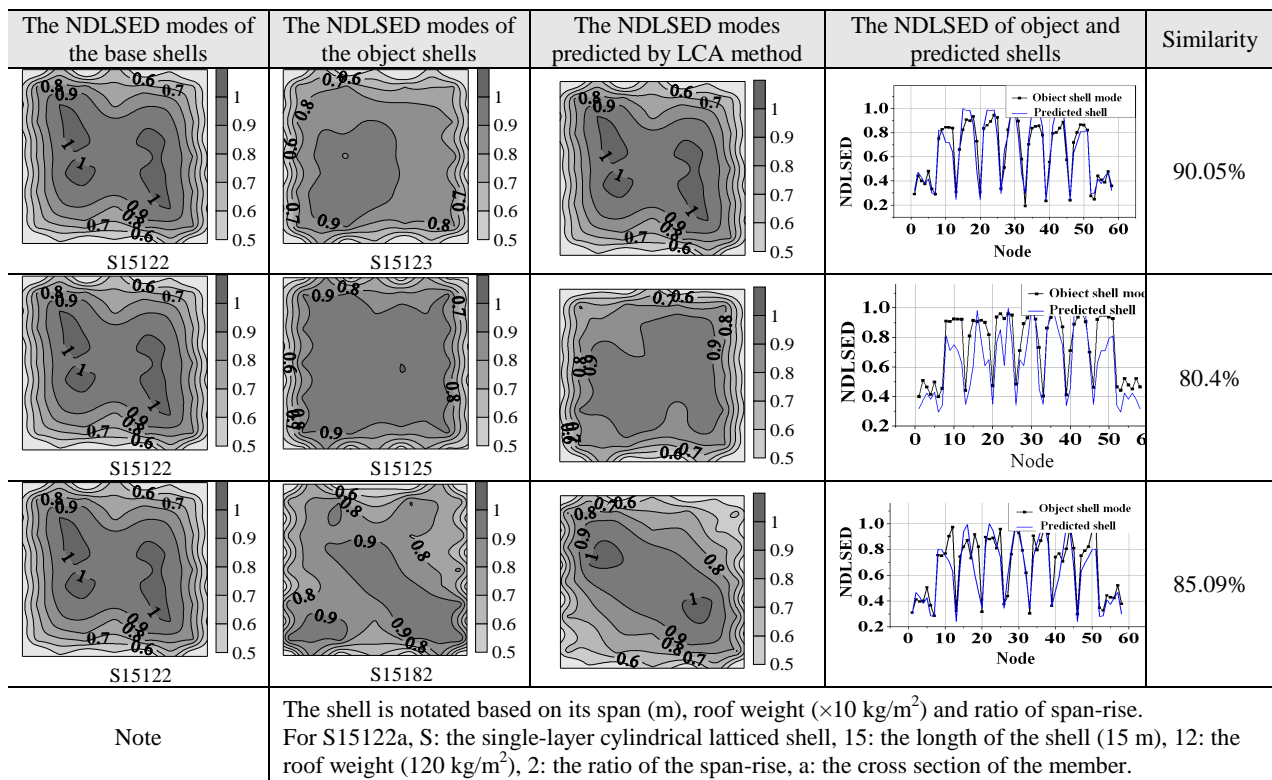


Figure 7. The strength failure modes of shells and comparison of mode similarity.

### 7 Conclusion

- (1) The LCA technique is applicable to modelling the configuration of a large-span single-layer shell. In the proposed LCA method, the concepts of nodal domain and nodal domain similarity as well as the criteria for matching nodal domain similarity and projecting the formative values of the base shell could reveal the relationship between the nodal domain similarity and the local working behaviour of the shell to an extent.
- (2) The LCA method further explores the application of the existing FEA (or testing) results and a new way to model the output of the FEA simulation.
- (3) The LCA method can save significant time in the prediction of the DF mode of the object shell when compared with the fine FEA method.
- (4) The LCA method is firstly applied to predict the strength failure mode of the single-layer shell based on the NDLSSED.

### Acknowledgements

The present work had the financial supports of the

Natural Science Foundation of China (No. 51278152) and the Fundamental Research Funds for the Central Universities (HIT. NSRIF. 2013113).

### References

- [1] Haruo, K., Koji, K.: *Response analysis of cylindrical roof shells subject to Kobe earthquake by mathematically analytic method*, Proceedings of Asia-Pacific Conference on Shell and Spatial Structures, Beijing China, 1996, 712-719.
- [2] Toshihiko, K., Takashi, O.: *Dynamic buckling behaviour of single layer latticed shells subjected to horizontal step wave*, Journal of the International Association for Shell and Spatial Structures, 44 (2003), 3, 167-174.
- [3] Shen, S. Z., Zhi, X. D.: *Failure mechanism of reticular shells subjected to dynamic actions*, China Civil Engineering Journal, 38 (2005), 1, 1-20. (in Chinese).
- [4] Zhi, X. D., Fan, F., Shen, S. Z.: *Elasto-plastic instability of single-layer reticulated shells under dynamic actions*, Thin-Walled Structures, 48 (2010), 10-11, 837-845.

- 
- [5] Du, W. F., Yu, F. D., Zhou, Z. Y.: *Dynamic stability analysis of K8 single layer latticed shell structures suffered from earthquakes*, Applied Mechanics and Materials, 2011, 94-96, 52-56.
- [6] Zhou, G. C., Rafiq, M. Y., Bugmann, G., Easterbrook, D. J.: *Cellular automata model for predicting the failure pattern of laterally loaded masonry panels*, Journal of Computing in Civil Engineering, ASCE, 20 (2006), 6, 400-409.
- [7] Neumann, J. V.: *The Theory of Self-Reproducing Automata*, University of Illinois Press Champaign, Chicago, 1996.
- [8] Toffoli, T., Margolus, N.: *Cellular Automata Machines: A New Environment for Modeling*, MIT Press, Cambridge, 1987.
- [9] Zhang, Y., Zhou, G. C., Xiong, Y., Rafiq, M. Y.: *Techniques for predicting cracking pattern of masonry wallet using artificial neural networks and cellular automata*, Journal of Computing in Civil Engineering, ASCE, 24 (2010), 2, 161-172.
- [10] Jen, E.: *Linear Cellular Automata and Recurring Sequences in Finite Fields*, Communications in Mathematical Physics, 119 (1988), 1, 13-28.
- [11] Chopra, A. K.: *Dynamics of structures theory and applications to earthquake engineering*, Tsinghua University Press, Beijing, 2009.
- [12] Cormen H. T., Leiserson E. C., Rivest L. R., Stein, C.: *Introduction to Algorithms, third edition*, The MIT Press, Cambridge, 2009.